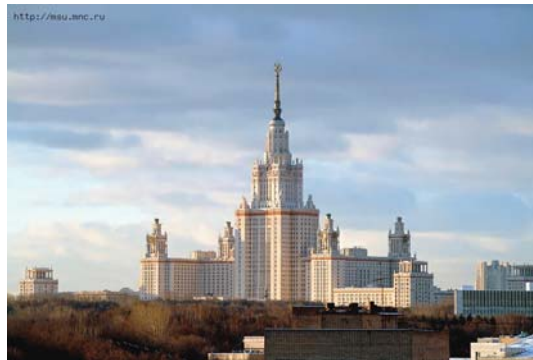


# $^{137}\text{Cs}$ and other radionuclides retention by geochemical and engineered barriers

Stepan N. Kalmykov

stepan@radio.chem.msu.ru

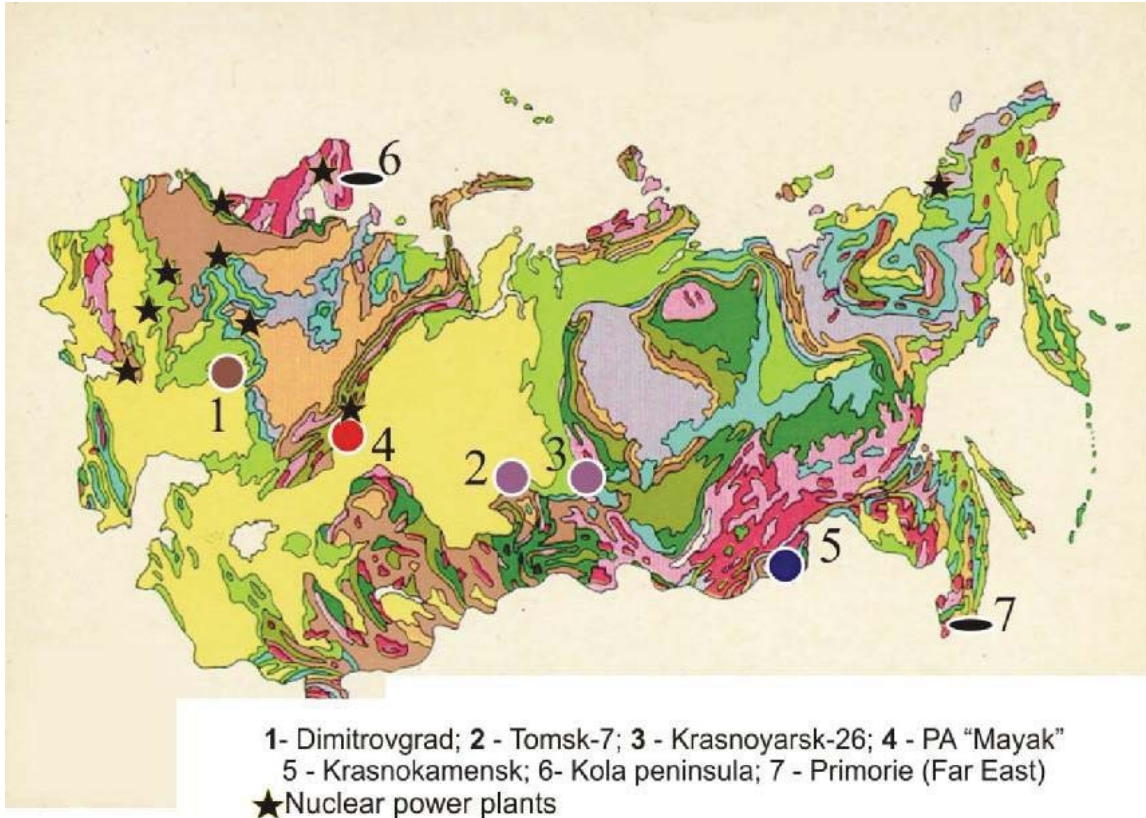


## Nuclear Russia

Source	Volume (m <sup>3</sup> )	Activity (Ci)
Uranium ore mining and treatment	10 <sup>8</sup>	1,8×10 <sup>5</sup>
Isotope enrichment and fuel production	1,6 × 10 <sup>6</sup>	4 × 10 <sup>4</sup>
Nuclear power stations	3 × 10 <sup>5</sup>	2,5 × 10 <sup>3</sup>
Radiochemical enterprises activities	5 × 10 <sup>8</sup>	9 × 10 <sup>8</sup>
Submarine and ice-boat operation	2,9 × 10 <sup>4</sup>	2,1 × 10 <sup>4</sup>
Submarine utilization	4 × 10 <sup>3</sup>	2 × 10 <sup>2</sup>
Isotope sources	2,0 × 10 <sup>5</sup>	6,0 × 10 <sup>2</sup>

As a result more than **600 Mm<sup>3</sup>** of nuclear wastes were accumulated with total activity of **2.5 billion Ci**

# Nuclear Russia



## Radionuclide speciation and local (nanoscale) distribution in samples collected at the contaminated sites

Techniques available in MSU:

UHR TEM (JEOL 2500),

$\mu$ -XPS, Auger and SIMS (Kratos),

XAFS (2.5 GeV line at Kurchatov Institute in Moscow ),

TRLIF

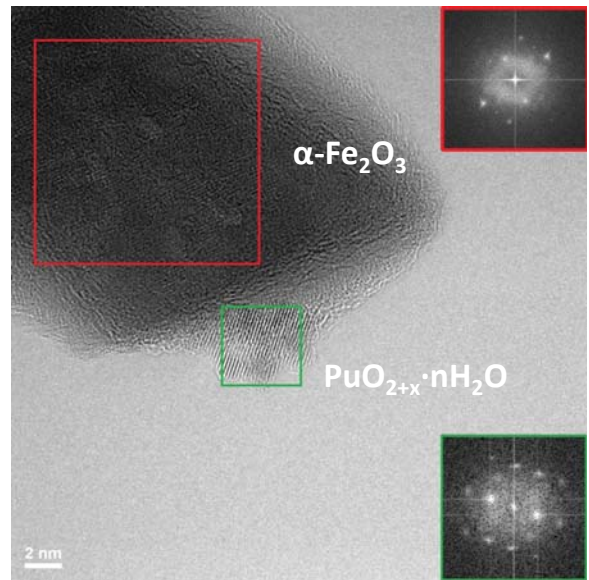
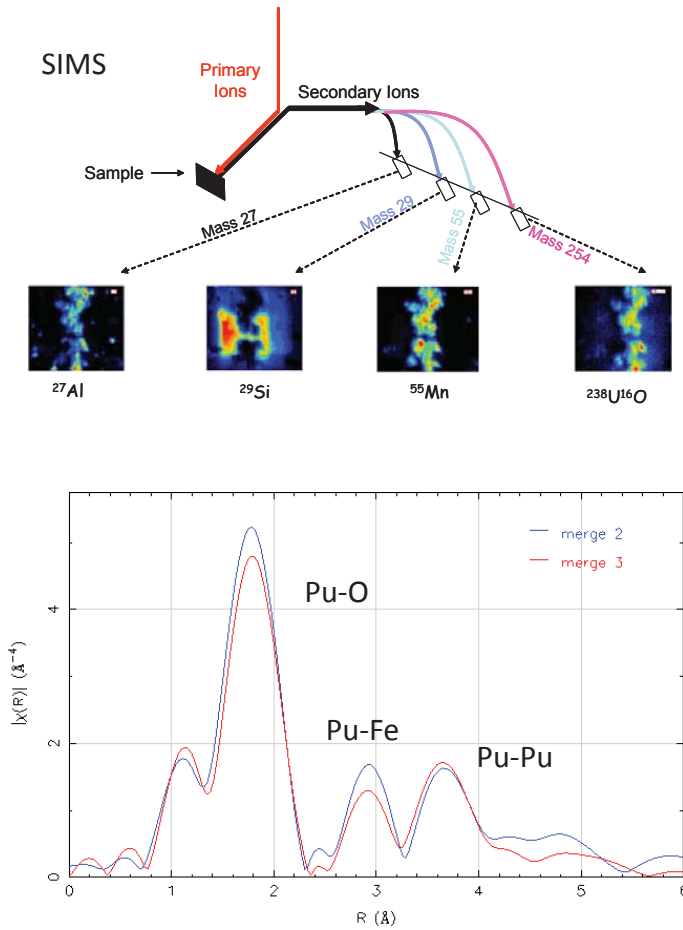
additionally:

Nanosizer Nano-ZS (Malvern),

SIMS,

SAXS, etc.

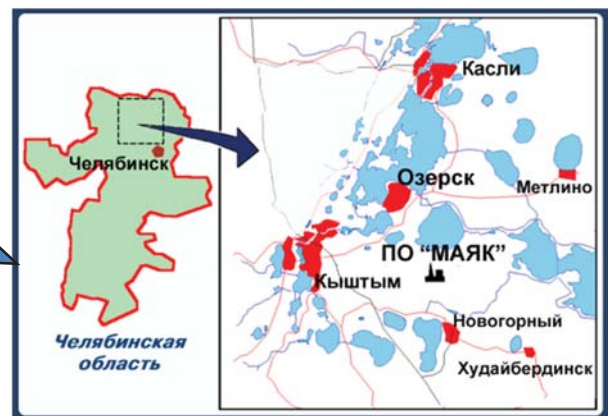
Alpha- track and fission track analysis



HR TEM

EXAFS

## Sources of radioactive contamination of South Ural



Dec. 22, 1948 – the plant to separate weapon grade Pu from irradiated uranium was launched

Production capacity was around 1 ton of U blocks per day

**about  $10^5$  Ci of wastes**

Year before the plant was launched, complex “C” was constructed that is the assembly of tanks for HLW. The capacity was estimated around **15000 m<sup>3</sup> per year**. However the real volume of wastes was **200 m<sup>3</sup> per day**.

All tanks were filled with HLW before 1950 (about a year after the plant was launched). The construction of new tanks for HLW was too expensive.

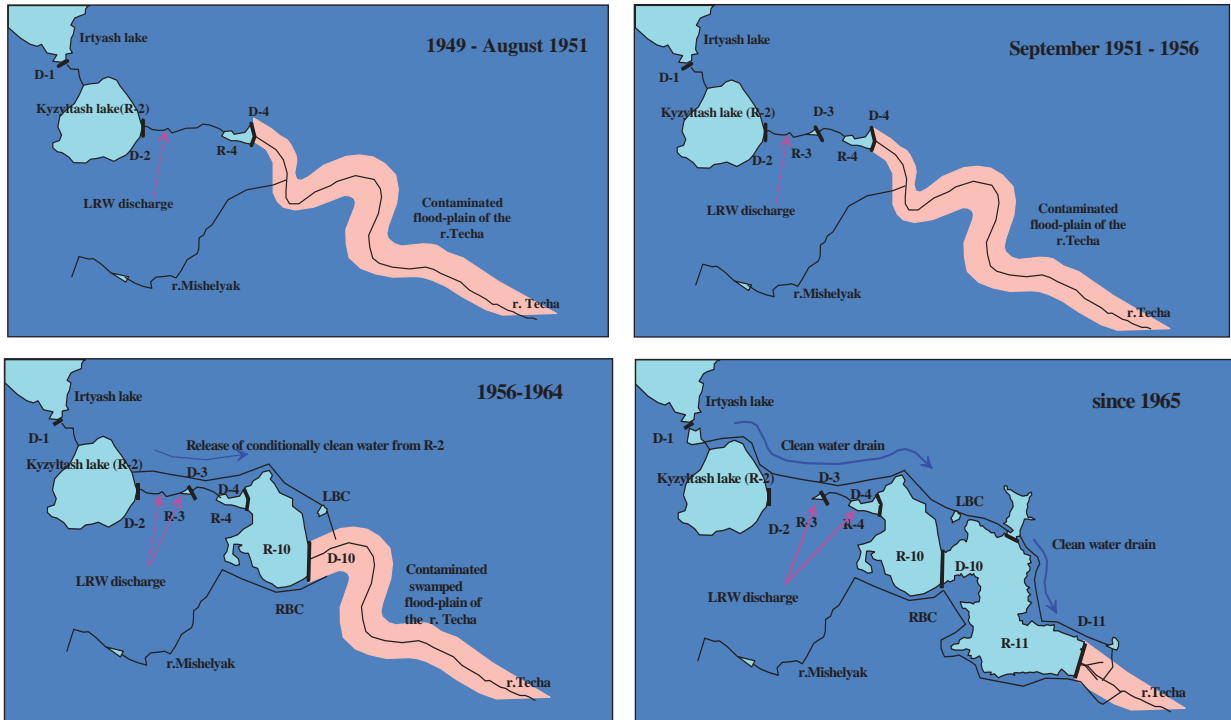
From 1949 till 1951 wastes were disposed to Techa river. During this period c.a. **76 Mm<sup>3</sup>** of waste solutions were disposed equal to 2.8 MCi.



## Volume of waste disposed to Techa river

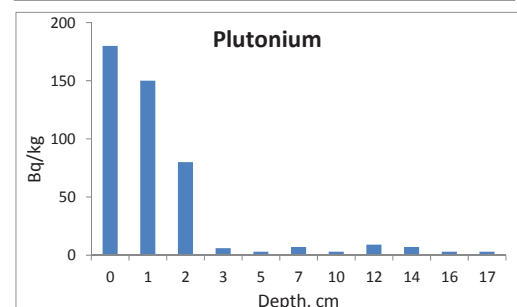
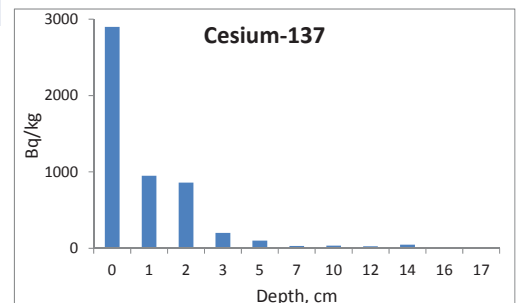
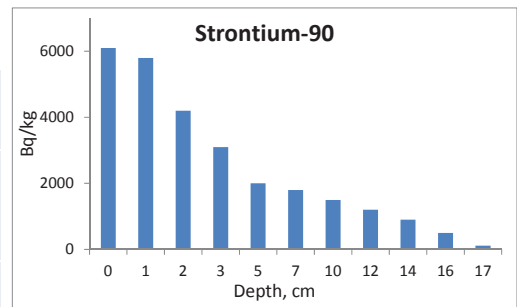
	I-XI.1949	XII.1949 -II.1950	III.1950 -XI.1951
Total β-activity, Ci/day	70	860	4300
<sup>89</sup> Sr + <sup>140</sup> Ba, %	1.8	6.9	8.8
<sup>90</sup> Sr, %	4.1	15.3	11.6
<sup>95</sup> Zr + <sup>95</sup> Nb, %	30	9.0	13.6
<sup>103,106</sup> Ru, %	55.6	45.3	25.9
<sup>137</sup> Cs, %	11	21.2	12.2
REE, %	-	5.7	26.8

# Creation of Techa cascade of reservoirs



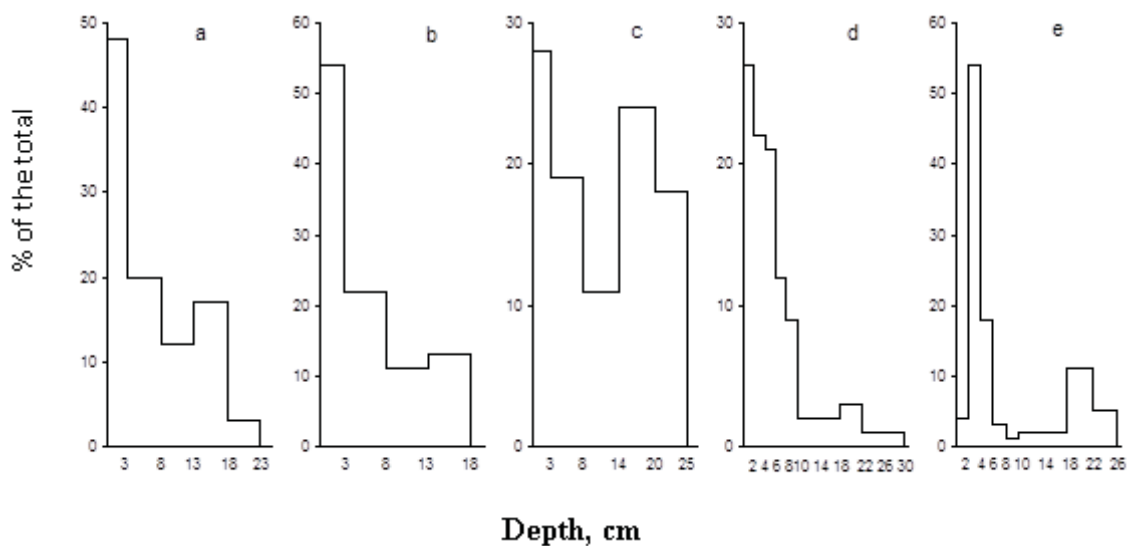
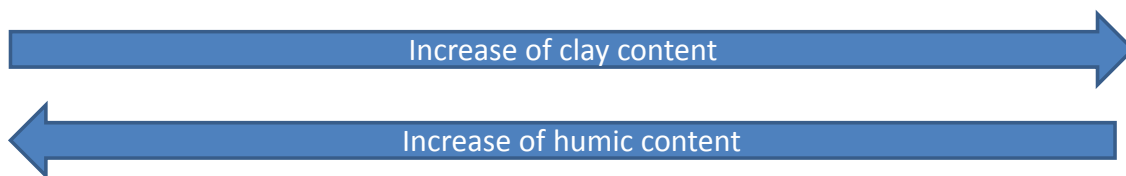
Contamination of flood plain soils, kBq/m<sup>2</sup>.

Location	<sup>90</sup> Sr	<sup>137</sup> Cs	<sup>239,240</sup> Pu
Right bank	61-750	18-1200	0,2-16,4
Left bank	20-220	15-270	0,3-2,0

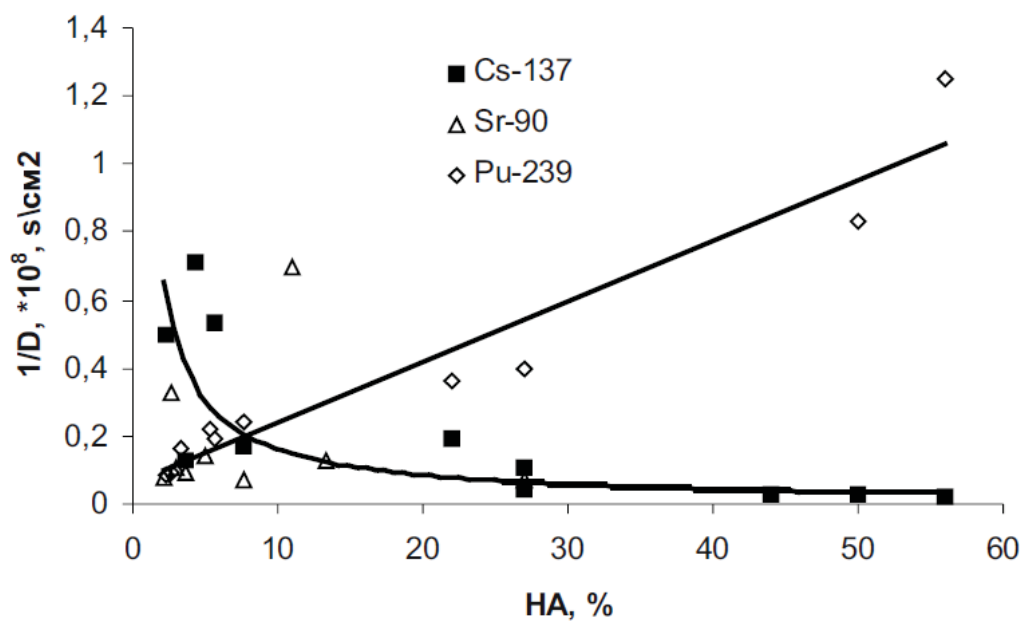


**Cs binding:**  
**Competition between**  
**clays and organic matter**

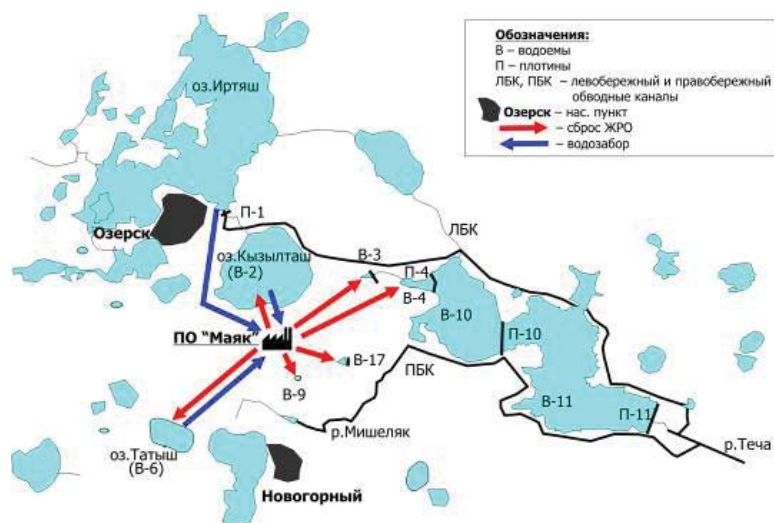
## Cs-137 distribution with soil types



## The dependence of diffusion resistance of various soils to $^{137}\text{Cs}$ , $^{90}\text{Sr}$ and $^{239}\text{Pu}$ vertical migration upon HAs concentration

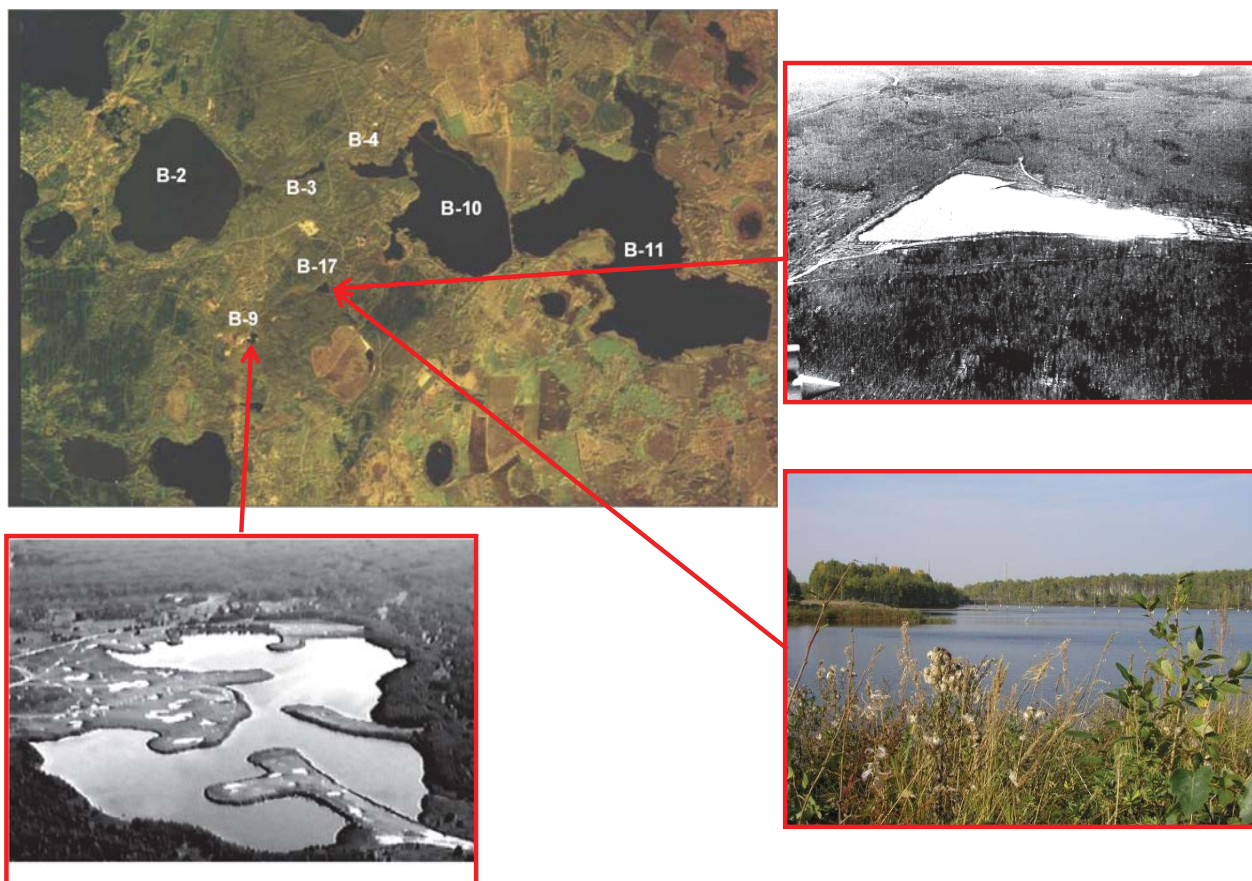


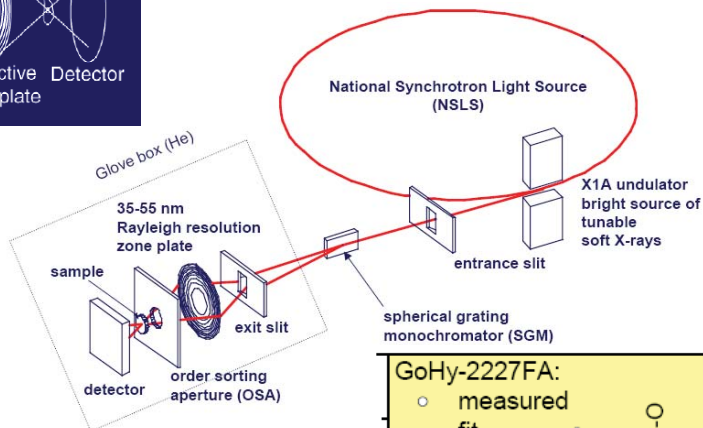
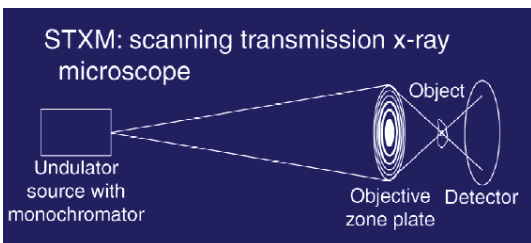
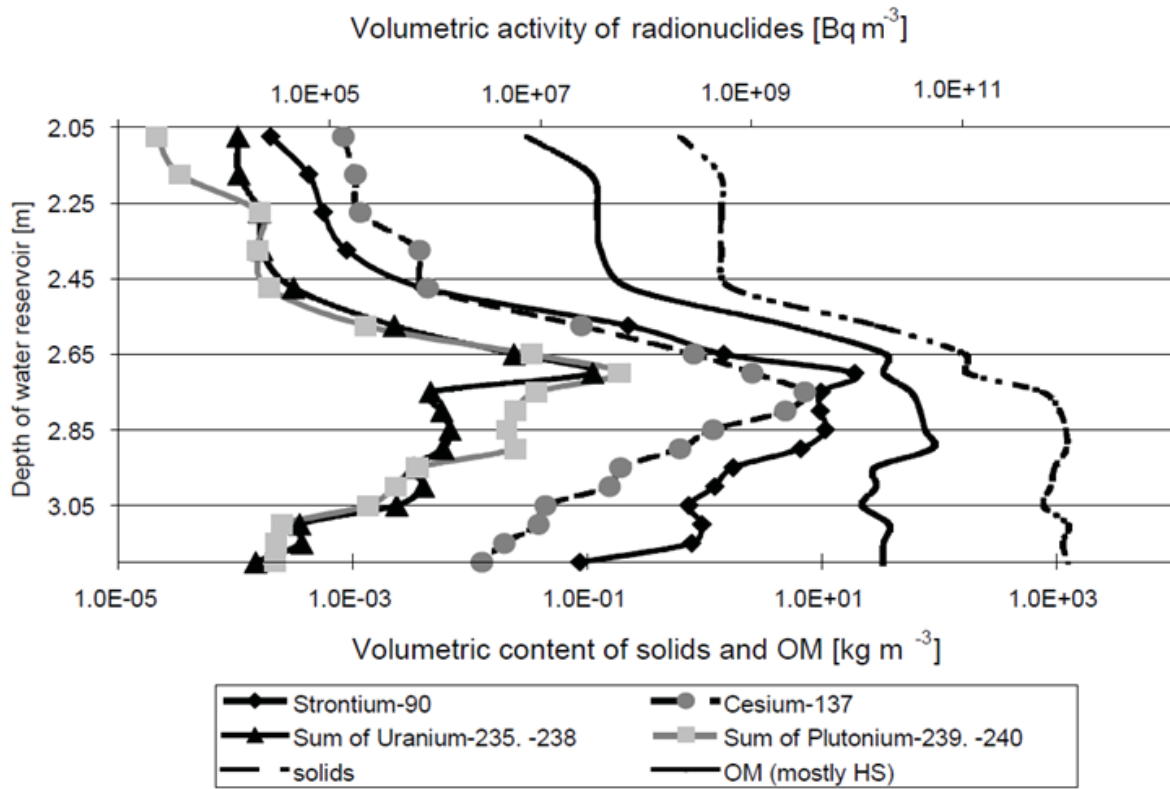
## Industrial reservoirs at “Mayak” site



In 1951 the disposal of wastes to Tеча was stopped and changed to lake Karachay that don't have connection with open hydrological system. LLW and ILW were also disposed to 8 artificial reservoirs: B-2 (lake Kiziltash), B-3, B-4, B-10, B-11, B-6, B-17 (called also Old Swamp) and B-9 (lake Karachay). About 120 MCi ( $4.4 \cdot 10^{18}$  Bq) of beta-emitters and 1 MCi ( $3.7 \cdot 10^{10}$  Bq) of alpha-emitters were disposed.

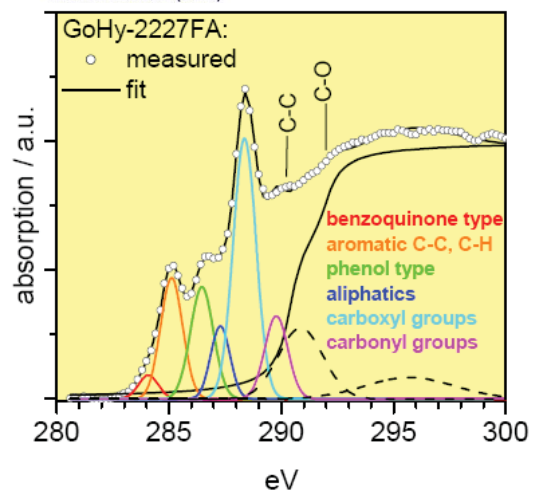
## Industrial reservoirs at PA “Mayak”





X1A1 (outboard): **C, K, Ca**  
 X1A2 (inboard): **(N), O, (Mn), Fe**

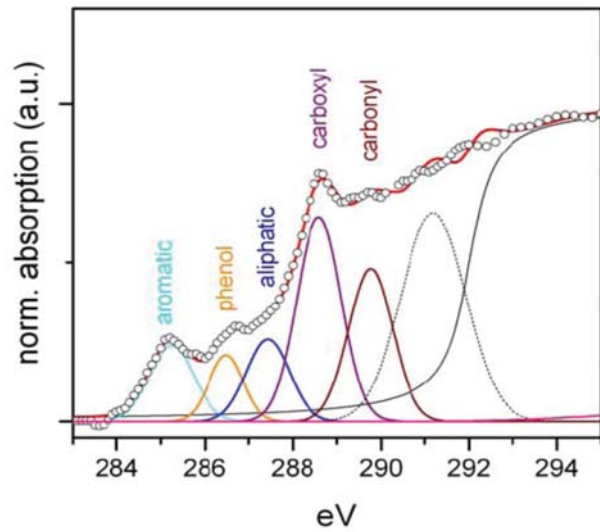
- **High spatial resolution:** 30-60 nm
- **Energy resolution:** 0.1-1.0 eV
- **Analysis without sample pretreatment**





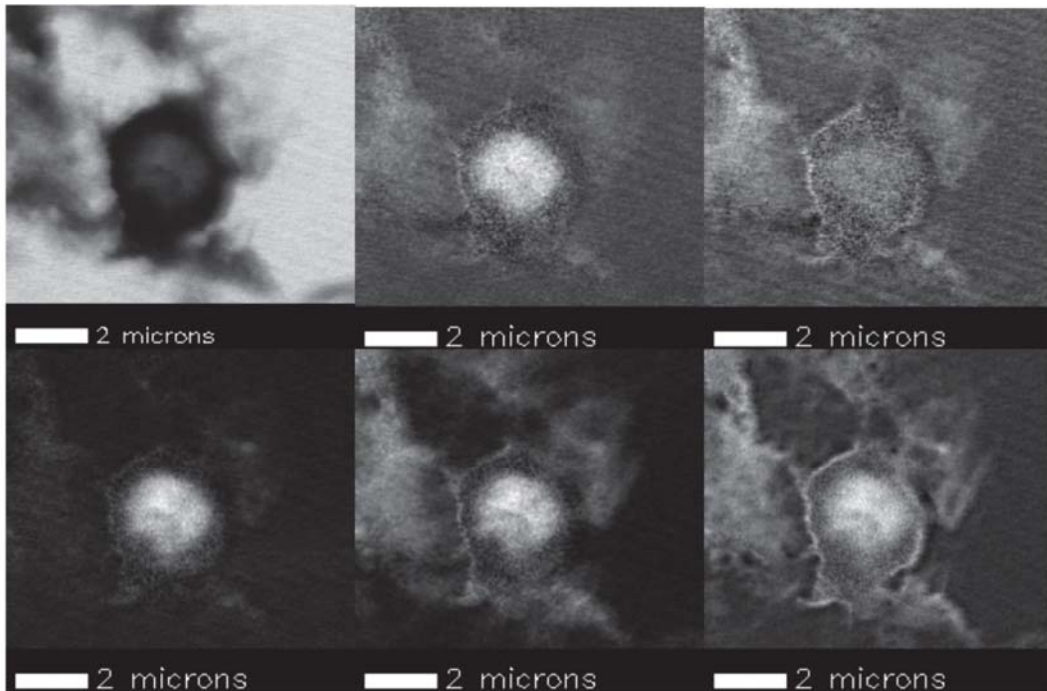
**Deconvolution of the average C1S spectra of humic-mineral aggregates**

Functional group	Content, %
C=C, C-H	14
Phenol	9
Aliphatic	15
Carboxyl	37
Carbonyl	25



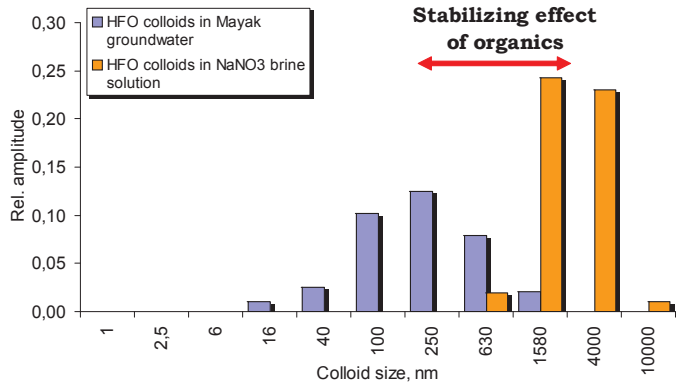
Deconvolution fit of sample with different carbon functionalities as indicated by the labels. The open dots represent the smoothed measured spectra obtained by cluster analysis and the red line indicated the fitted spectra

**STXM**

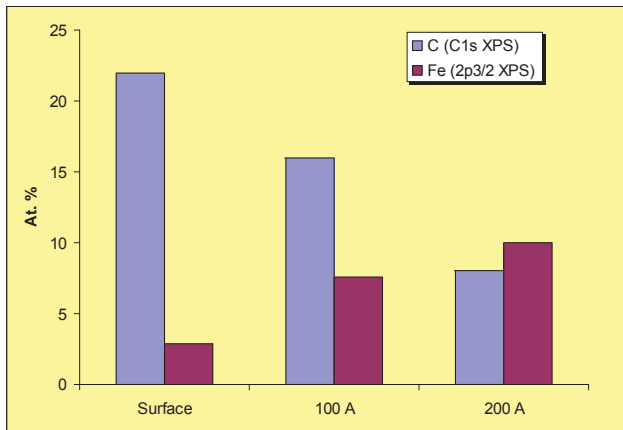
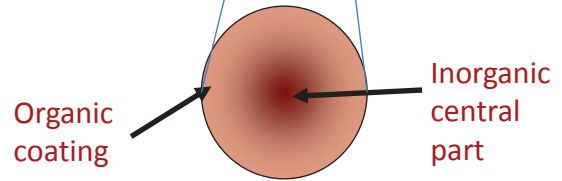
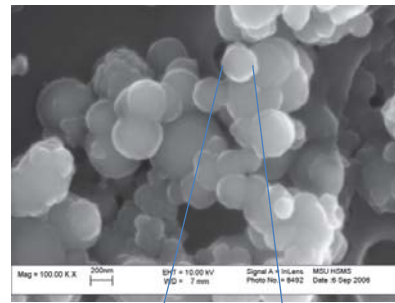


From left to right, upper row; absorption image at 280eV below the C1s edge; ratio images showing the distribution of aromatics, phenol-type groups and lower row aliphatics, carboxyl-type groups and total organics. Bright grey values indicate high concentrations of organic functionality

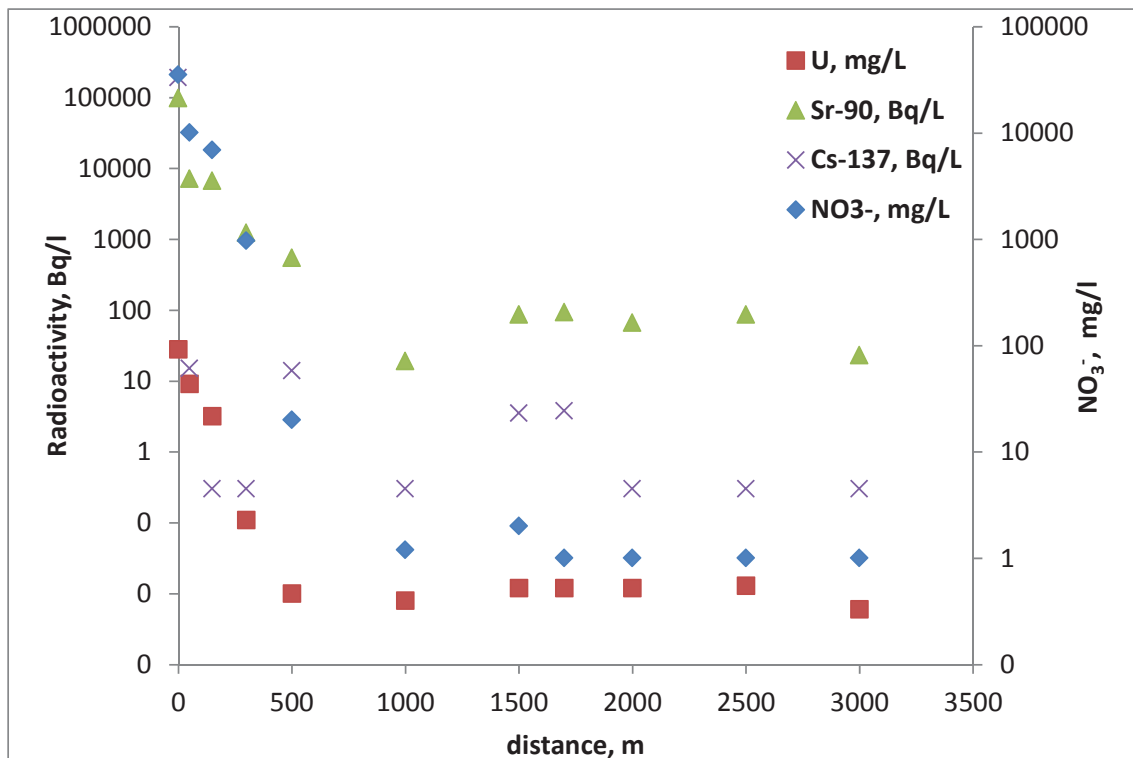
# Effect of organics on colloid particle stability



XPS, Auger microscopy with ion etching



# Penetration of various radionuclides and NO<sub>3</sub><sup>-</sup> by geological media



# Approaches for barriers design

Bentonite clays

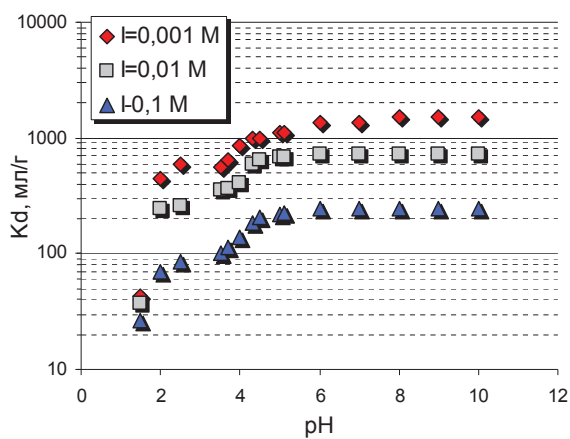
Immobilized humic derivatives

Carbon nanomaterials

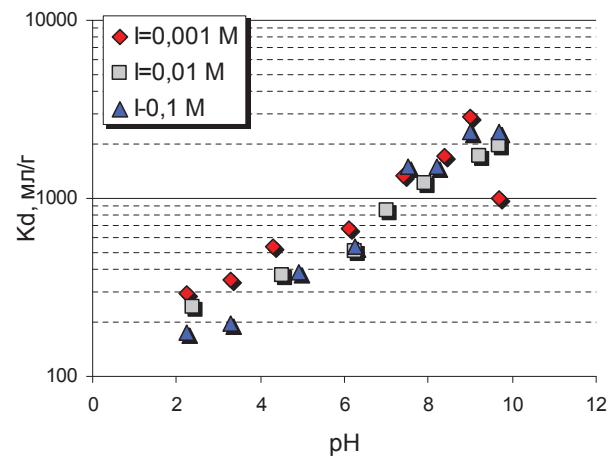
## Khakassiya bentonite

Mineral	Weight concentration, %
Montmorillonite	70–80
Quartz and kristobalite	10–12
Albite	4–6
Calcite	2–3
Hematite and magemite	<2
Pirofilite	1–2

Cs(I) sorption onto bentonite

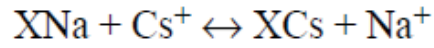


Np(V) sorption onto bentonite



# Khakassiya bentonite

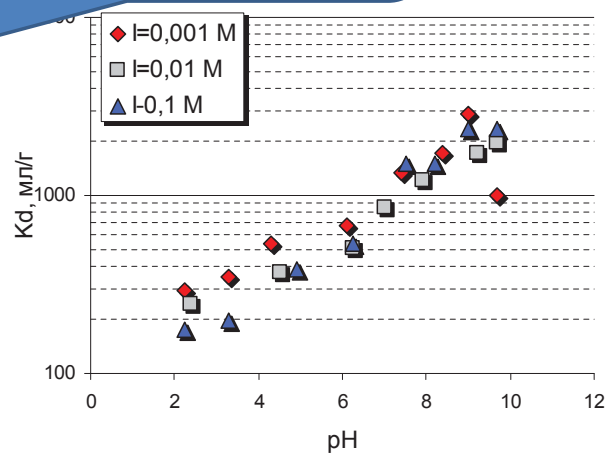
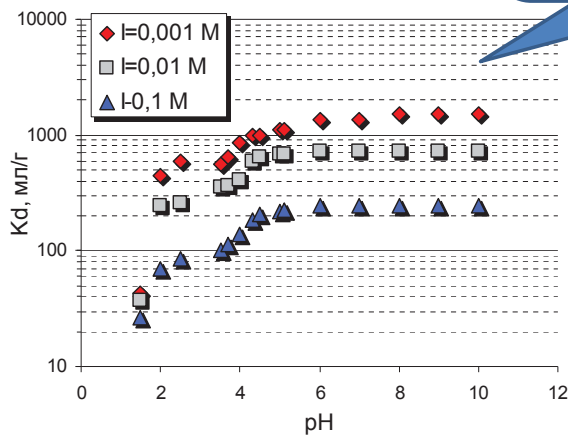
Mineral	Weight concentration, %
Montmorillonite	70–80
Quartz and kristobalite	10–12
Albite	
Calcite	
Hematite and magemit	
Pirofilite	



$$\log K_{ie} = 1.7$$

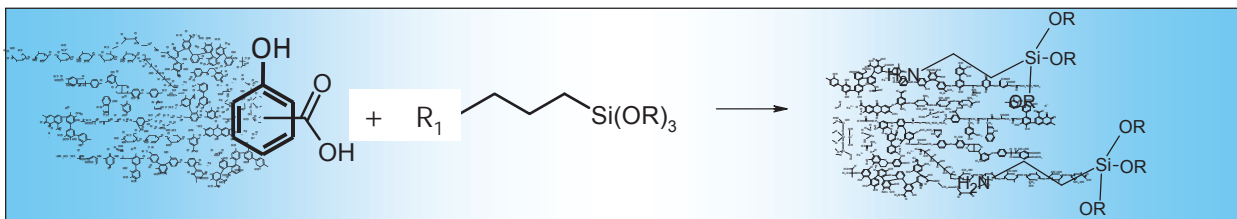
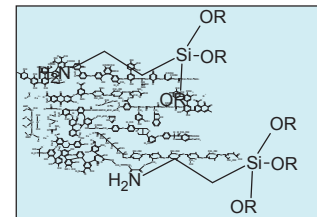
Cs(I) sorption onto bentonite

bentonite

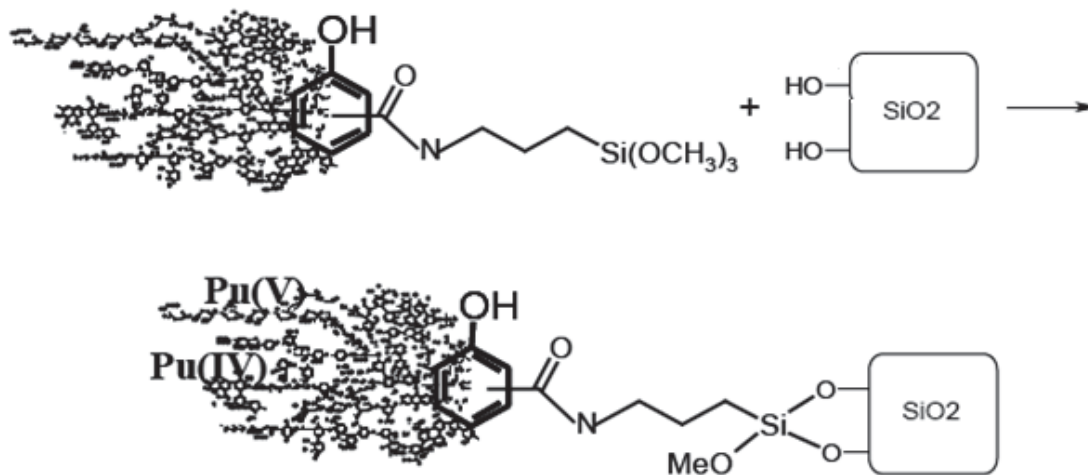


In collaboration with Irina Perminova, MSU

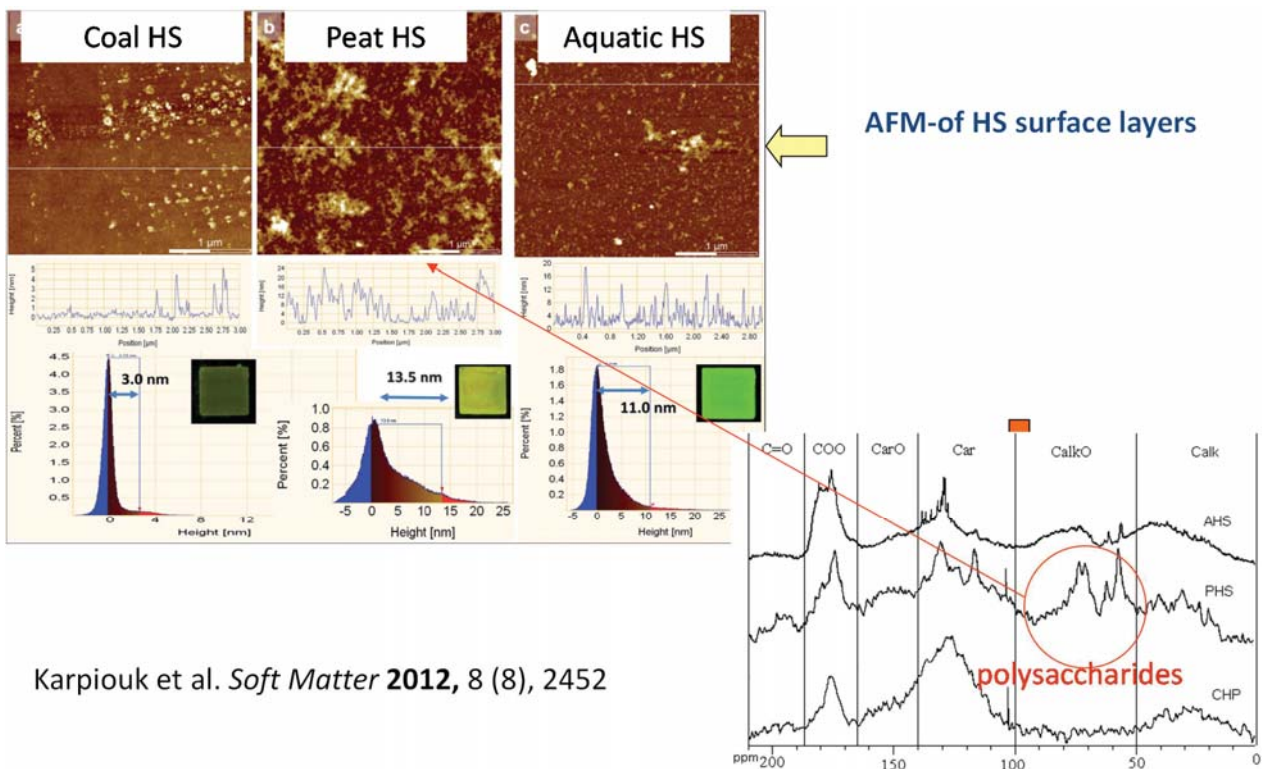
## Preparation of alkoxylenated derivatives of humic acids with various organosilans



R <sub>1</sub>	Organosilan	Structure
<b>Amino</b>	3-aminopropyl-trialkoxysilane (APTS)	$H_2N(CH_2)_3Si(OR)_3$
<b>Epoxy</b>	3-glycidoxypropyl-trialkoxysilane (GPTS)	
<b>Isocyanate</b>	3-isocyanatopropyl-trialkoxysilane (IPTS)	$OCN(CH_2)_3Si(OR)_3$

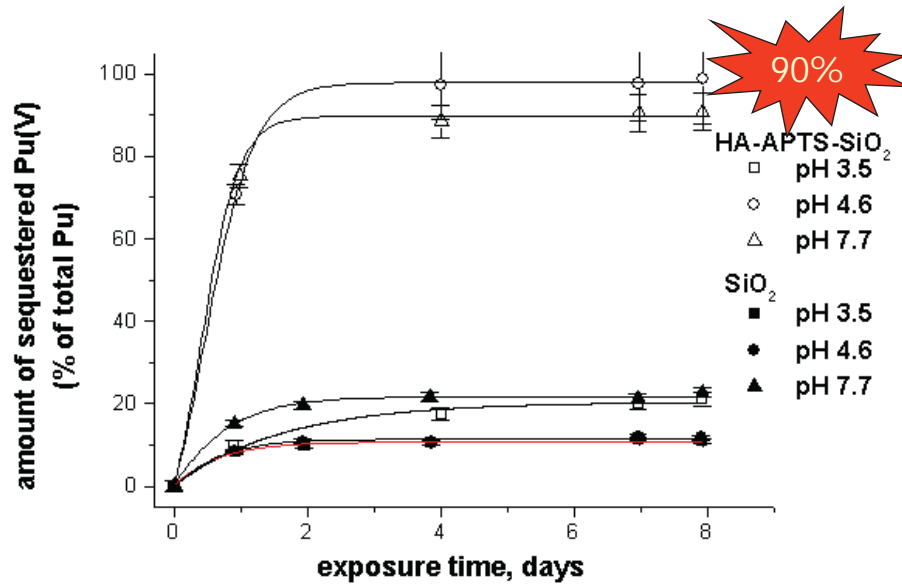


## Humic sorbents on SiO<sub>2</sub> support

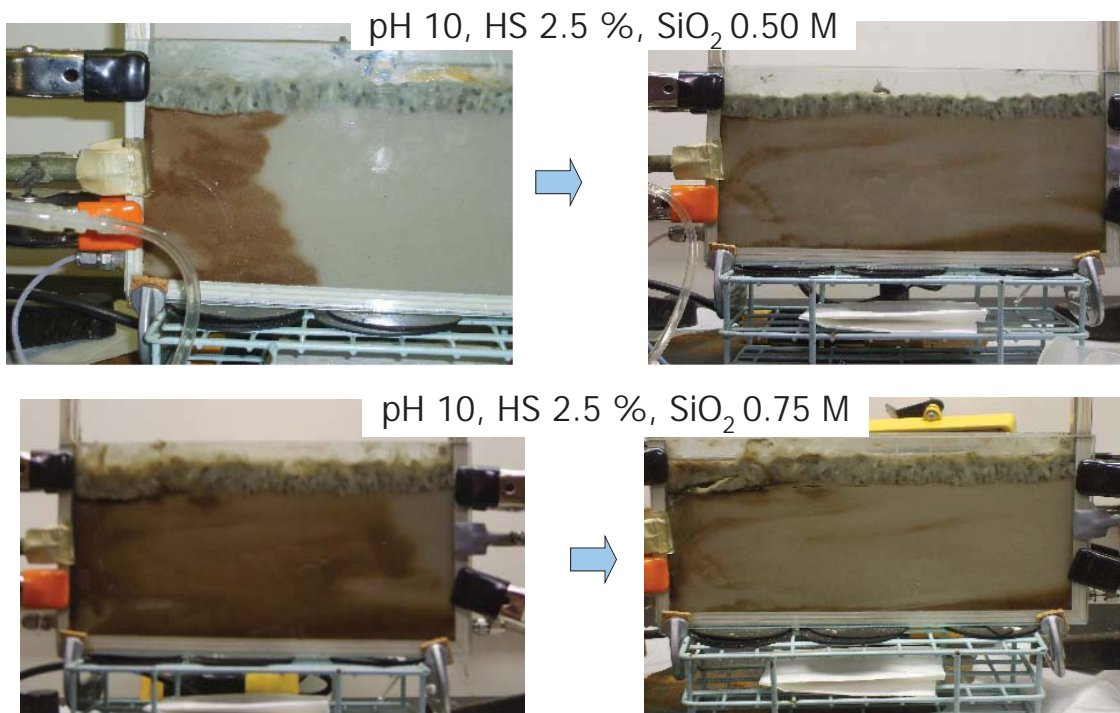


Karpiouk et al. *Soft Matter* **2012**, 8 (8), 2452

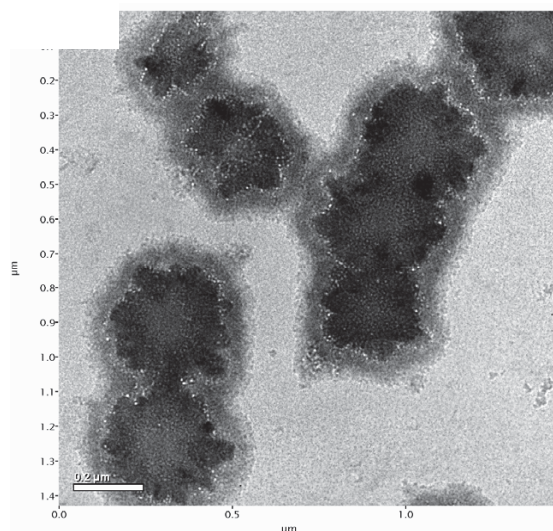
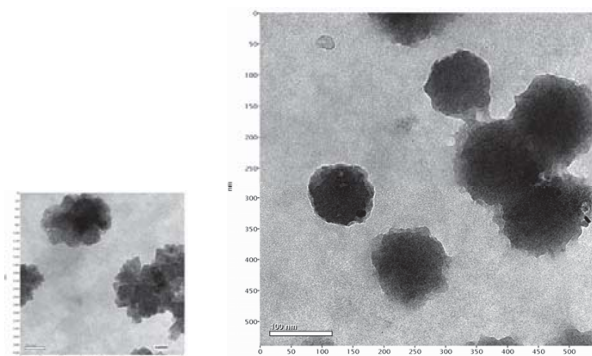
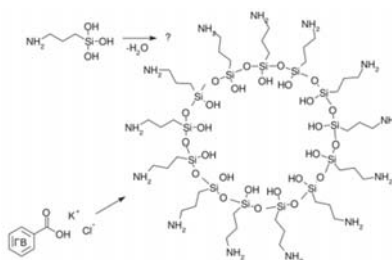
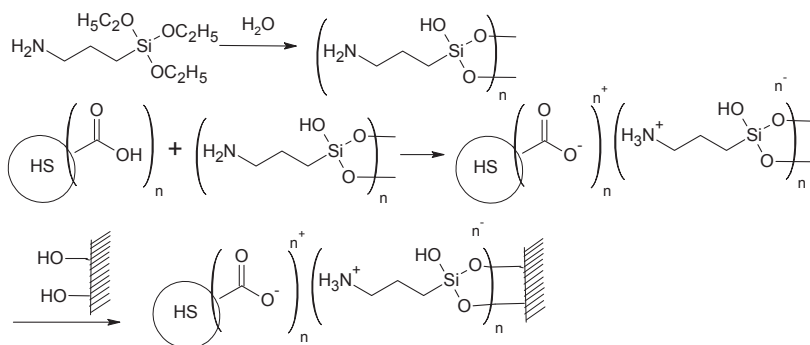
## Example: Pu sorption



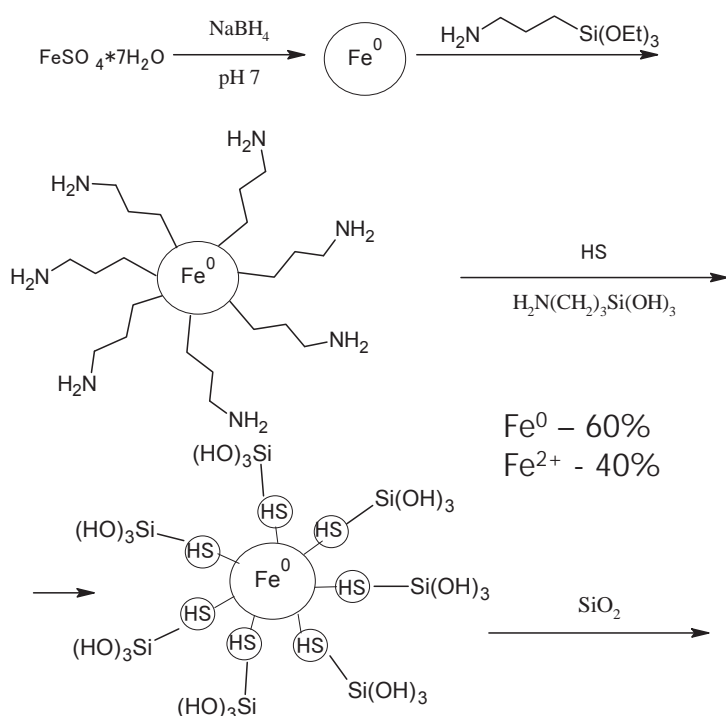
## Simulation of permeable reaction barrier



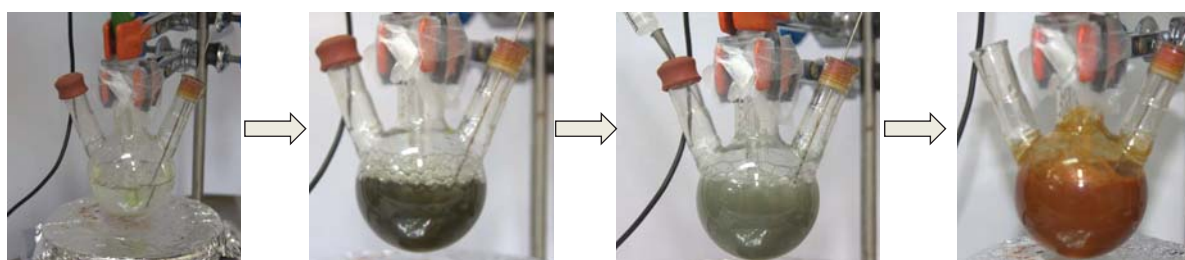
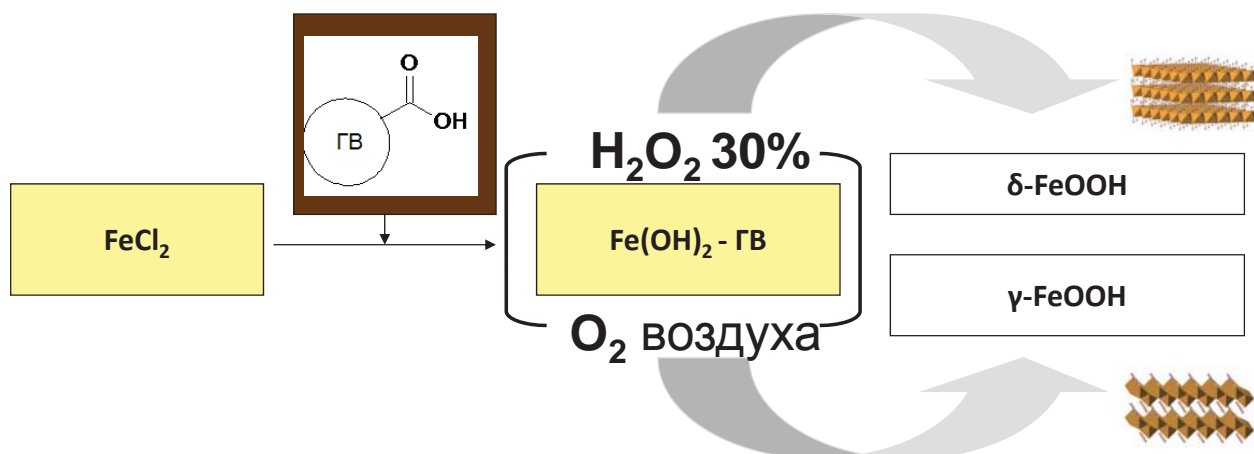
## Aminoorganosilane – formation of micelles



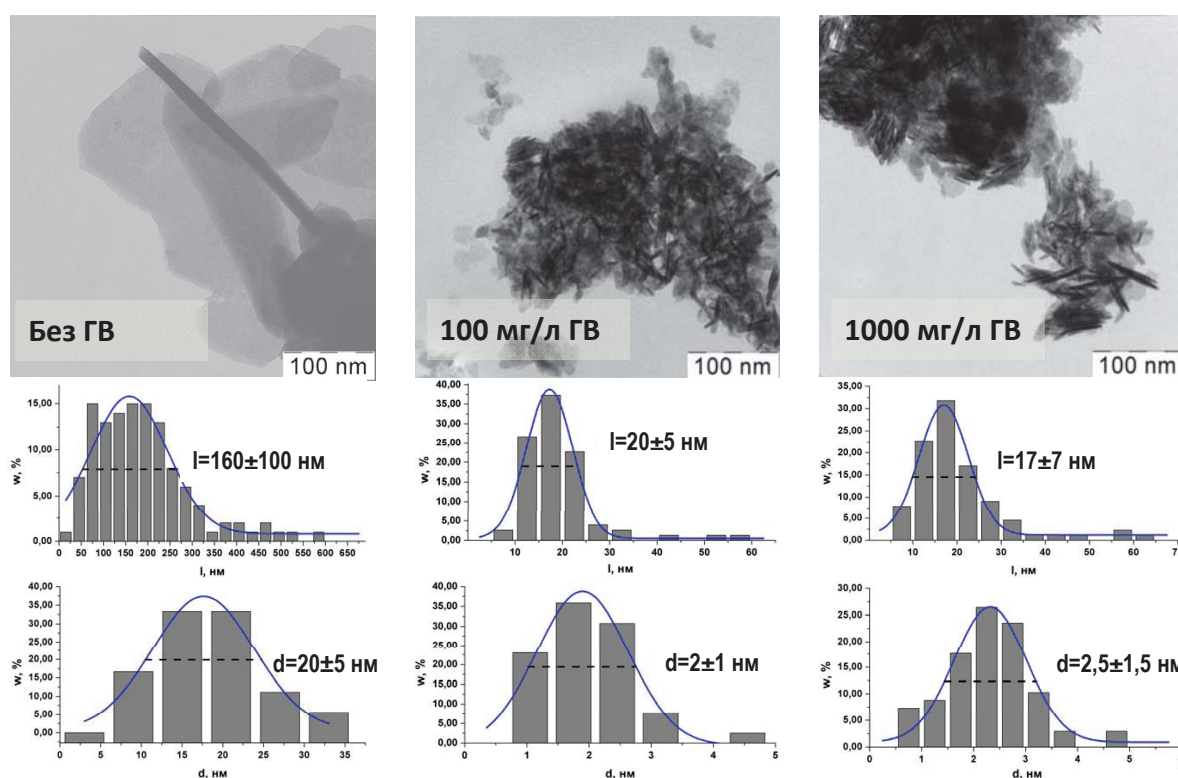
## Stabilization of zero valent Fe nanoparticles by HS



## Iron oxides nanoparticles stabilized by HS

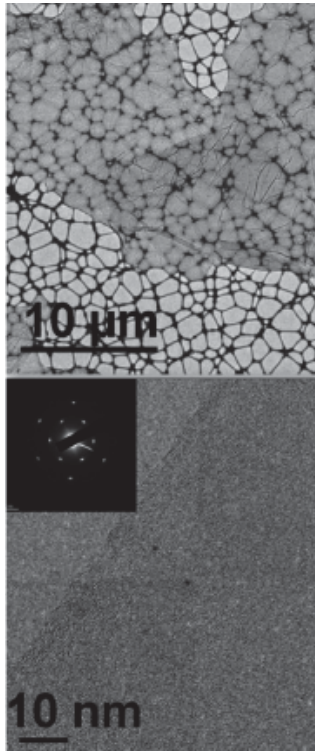


## Formation of $\delta\text{-FeOOH}$ in the presence of HS





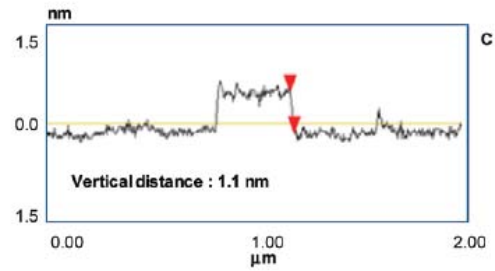
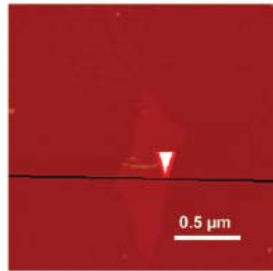
## Carbon nanomaterials as effective scavengers for radionuclides



### Graphene oxide

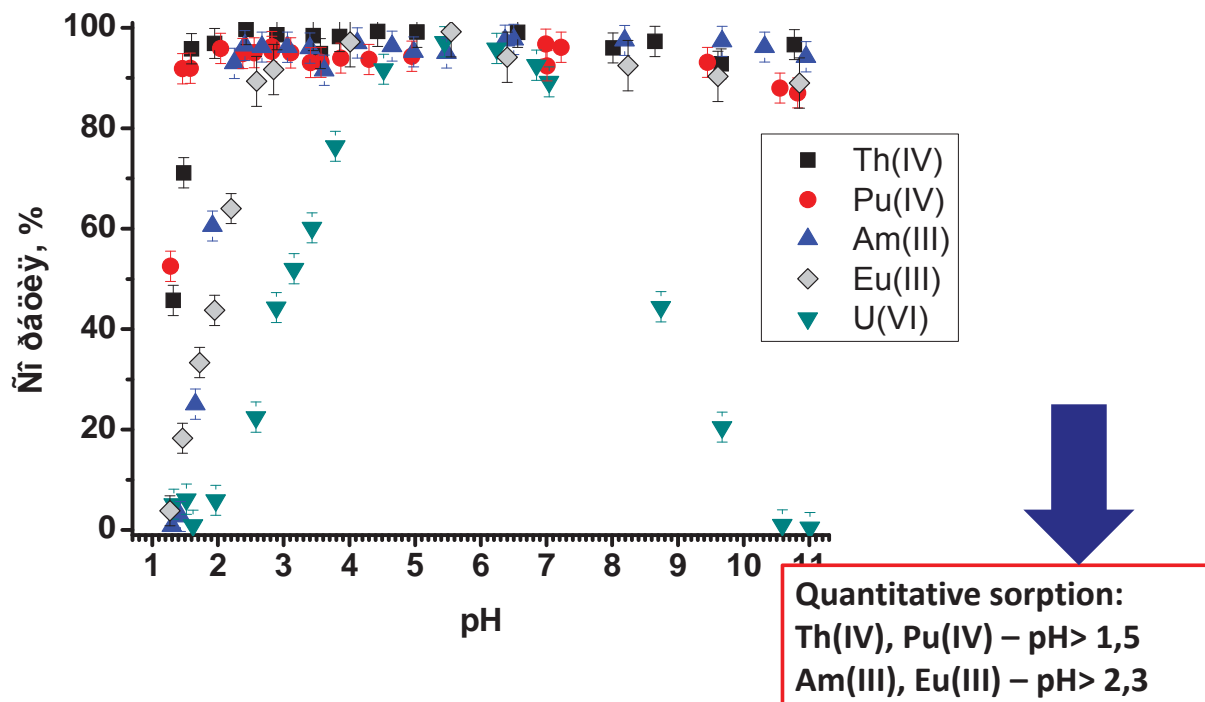
Hummer modified method

Graphite +  $\text{KMnO}_4$   
9:1  $\text{H}_2\text{SO}_4$  и  $\text{H}_3\text{PO}_3$



Marcano et al., ACS Nano, 2010

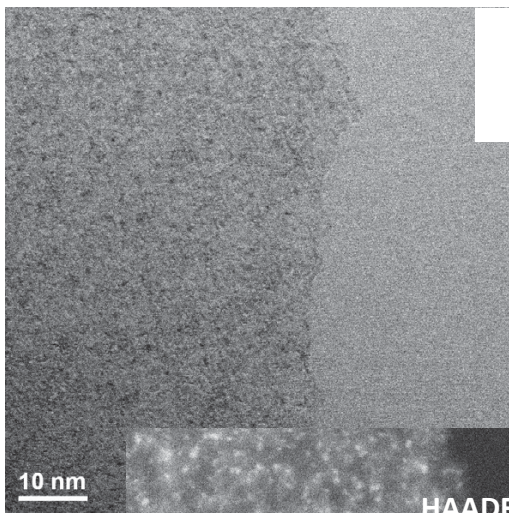
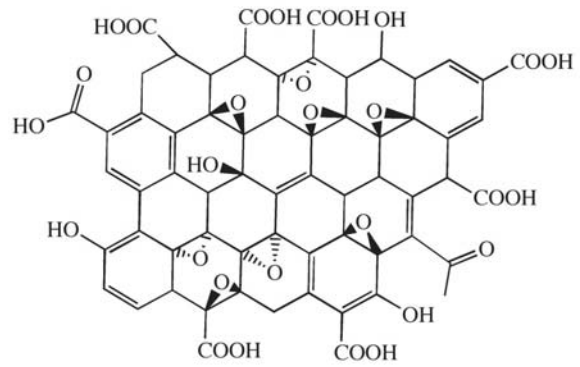
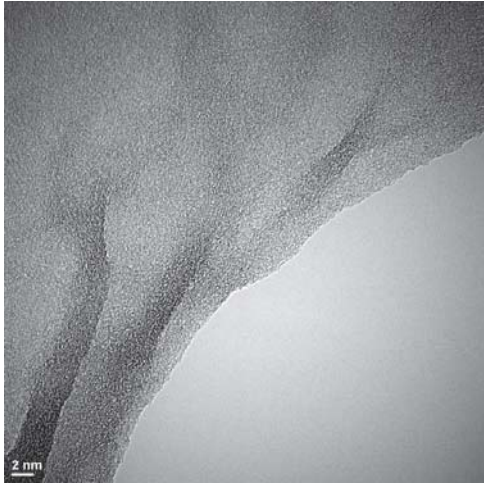
## Earlier the effective scavenging of actinides and lanthanides was shown



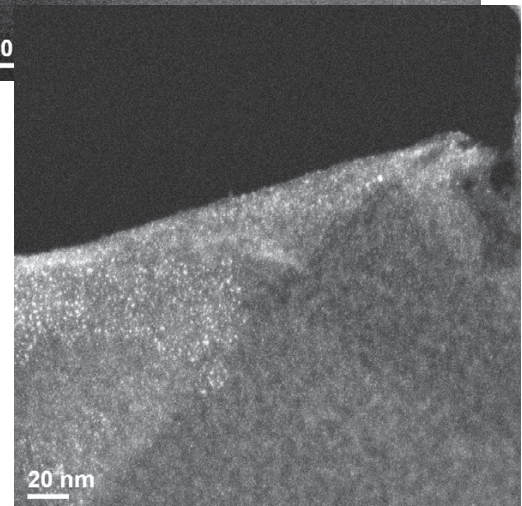
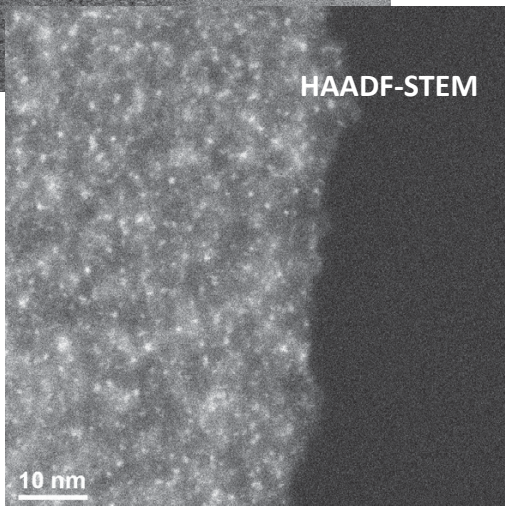
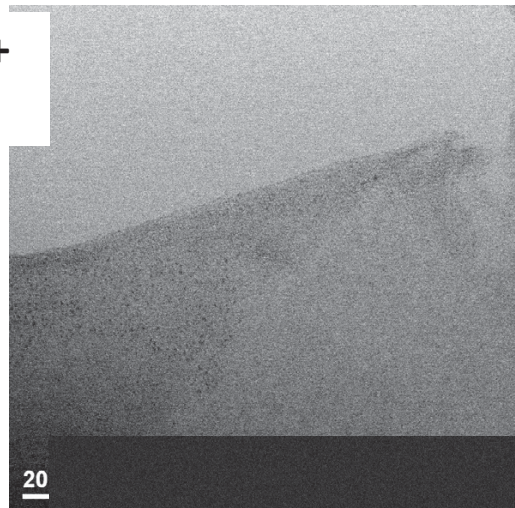
	$Q_{\text{max}}$ , мкмоль/г
U(VI), pH = 3,5	97 ± 19
U(VI), pH = 5,0	116 ± 5
Sr(II), pH = 6,5	272 ± 35
Cs(I), pH = 7,0	160 ± 75

## GO + Cs(I)

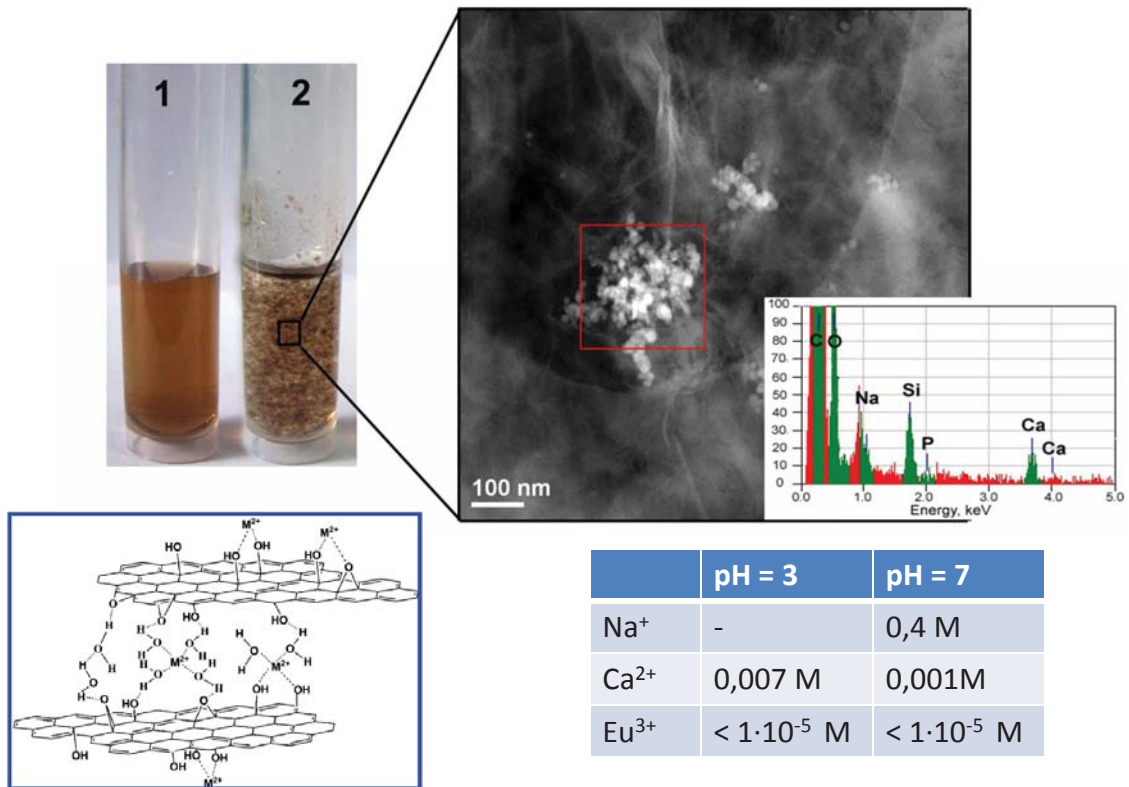
Distribution of Cs(I)  
on the surface



Cations +  
GO



# Coagulation of GO



## Conclusions:

1. As expected, clays effectively sorb Cs<sup>+</sup>, but the presence of humic could change the mobility of Cs<sup>+</sup>,
2. Humics form stable surface coatings on mineral particles that change their sorption and coagulation properties,
3. Humics could be easily modified and immobilized onto silica surfaces, as a result permeable barrier could be formed,
4. Graphene oxide could be considered as an effective scavenger for cationic forms of radionuclides.